

# HIGH QUANTUM EFFICIENCY ALKALI-ANTIMONIDE PHOTOCATHODES FOR PERLE HIGH CURRENT DC GUN\*

M. De Vos<sup>†</sup>, S. Brault, J. Demailly, O. Frossard, T. Gerardin, W. Kaabi, B. Mercier, E. Mistretta, D. Reynet, J. Yemane, G. Sattonnay, Université Paris-Saclay, CNRS/IN2P3, IJCLab, Orsay, France  
M. Baylac, Laboratoire de Physique Subatomique et de Cosmologie, Grenoble, France

M. Faye, Grand Accélérateur National d'Ions Lourds, Caen, France  
On behalf of the PERLE collaboration

M. Hoffmann B. Keune, V. Kuemper, C. Quitmann, RI Research Instruments GmbH, Bergisch Gladbach, Germany

## Abstract

Modern particle accelerators, while enabling cutting-edge research, face major challenges in energy efficiency and beam intensity. The PERLE (Powerful Energy Recovery Linac for Experiments) project, developed at IJCLab/CNRS, aims to demonstrate a high-current energy recovery linac (ERL) using superconducting RF technology. By recovering the beam energy after use, PERLE drastically reduces RF power consumption, paving the way for sustainable, high-performance accelerators. A key element is the development of alkali-antimonide photocathodes, combining high quantum efficiency and low thermal emittance. CsK<sub>2</sub>Sb photocathodes, in particular, show excellent response to visible light, enabling operation with lower laser power and improved beam quality. Their fabrication relies on a unique deposition system equipped with a dedicated transfer line that links the glove box—where precursors are prepared—to the molecular beam epitaxy (MBE) chamber for growth, and ultimately to the electron gun for installation. First tests at IJCLab achieved a quantum efficiency of 7 %, validating this integrated approach for high-current ERLs such as PERLE.

## INTRODUCTION

High-performance electron sources are essential for modern accelerator facilities such as energy recovery linacs (ERLs) and X-ray free-electron lasers (XFELs). These applications require photocathodes capable of delivering high brightness beam at fast time response, low thermal emittance and stable operation [1]. For that, alkali antimonide photocathodes, in particular CsK<sub>2</sub>Sb, are widely considered promising candidates due to their high quantum efficiency (QE) in the visible range and their compatibility with high-current operation [2].

However, the performance and lifetime of these photocathodes are strongly influenced by vacuum conditions during growth and operation. Residual gases, such as O<sub>2</sub> and CO<sub>2</sub>, can affect the formation of the photocathode, its stoichiometry and contribute to rapid degradation of the quantum efficiency [3,4]. While optimized growth

procedures have been widely studied, including sequential and co-evaporation techniques [5,6], the impact of non-ideal vacuum conditions remains a critical practical issue for photocathode preparation systems.

In this paper, we present a comparative study of two CsK<sub>2</sub>Sb photocathodes prepared under different vacuum conditions. The results highlight the sensitivity of the growth process and the resulting photoemission properties to vacuum quality, providing insight into the requirements for reliable photocathode production in high-current accelerator environments such as PERLE.

## EXPERIMENTAL

### Photocathode Preparation Facility (PPF)

The photogun of PERLE is equipped with a Photocathode Preparation Facility (PPF) enabling the transfer of the photocathode under vacuum (Fig. 1) via a trolley. This includes a glovebox, where 2" diameter molybdenum or stainless-steel substrates (pucks) are loaded and where all the chemicals are used. The trolley is then inserted into the transfer line and automatically moved in front of the MBE chamber. One puck at a time can be inserted in the chamber for deposition. After deposition, the puck can be moved to the electron gun via the transfer line.

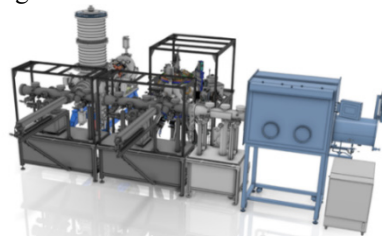


Figure 1: photocathode preparation facility (PPF) with glove box and MBE chamber connected to the photogun.

### Precursors Preparation

All precursors were used under argon atmosphere in the glovebox (Ar: 2 bars, O<sub>2</sub> < 5 ppm and H<sub>2</sub>O < 1 ppm). Antimony balls (Alfa Aesar, 99.9999 %) were melted in order to remove oxygen contamination inside an alumina crucible, ¼ filled. Potassium (Strem, 99 %) was melted and introduced into a molybdenum crucible. Then, a large excess (10 times) of indium (MaTeck, 99.9999 %) was added

\* Work supported by the *Agence Nationale de la Recherche* via its program ANR-24-RR11-0001  
<sup>†</sup>melanie.de-vos@ijclab.in2p3.fr

twice after melting, filling the crucible at  $\frac{1}{3}$ . The same procedure was performed for caesium (Ala Aesar, 99.98 %). The three crucibles, holding air-stable alloys, were finally removed from the glovebox and inserted into their respective effusion cells.

### MBE Preparation

The effusion cells were loaded in their respective evaporators. Note that Sb evaporator is a double-stage. Bake out was performed at 150 °C during 3 days before maintaining the evaporators at a standby temperature (150 °C and 250 °C for Sb, 210 °C for K and 220 °C for Cs). The puck inside the MBE chamber was also baked out, at 500 °C during 8 h, in order to remove any surface contamination. Then its temperature was decreased to 100 °C for the deposition process. It can be performed when the pressure is stable below  $10^{-8}$  mbar thanks to an ion pump equipped with a NEG and a turbo pump.

### Photocathode Preparation

The photocathode syntheses were performed according to a sequential deposition already investigated by *Research Instruments GmbH* [7]. First, antimony evaporator temperatures were increased up to 520 °C and 670 °C for the lower stage and upper stage respectively. A 20 nm layer of Sb was deposited on the stainless-steel puck. The deposition was continuously monitored and stopped according a quartz microbalance inside the MBE chamber (Fig. 2).

As a second step, the potassium evaporator temperature was increased up to 300 °C. Then the evaporation of K was monitored by measuring the quantum efficiency (QE). Its measurement is enabled by a green laser, hitting the puck centre, and a mask containing an anode biased at +200 V.

Finally, the caesium evaporator was increased up to 305 °C. The evaporation of Cs was also monitored by the QE measurement and stopped at the maximum.

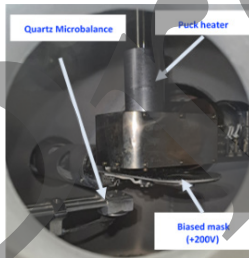


Figure 2: Photograph of the inner part of the MBE.

## RESULTS AND DISCUSSION

Two photocathodes were synthesized using the same deposition parameters. The MBE pressure, as well as the temperatures were monitored on the first hand. On the second hand, the photocurrent, thickness and QE were also measured.

The first photocathode revealed an undesired increase of pressure (Fig 3. a.). Indeed, the heating of the Sb evaporator generates outgassing responsible of a first increase from  $\sim 2 \cdot 10^{-8}$  to  $\sim 10^{-7}$  mbar [8]. Similar trends were observed during K and Cs evaporators heating, leading to increases from  $\sim 4 \cdot 10^{-8}$  to  $\sim 6 \cdot 10^{-7}$  mbar and from  $\sim 2 \cdot 10^{-7}$  to  $\sim 5 \cdot 10^{-7}$

mbar respectively. During the heating of Sb and K evaporators, the absolute value of photocurrent increased (Fig 3. b.). This is correlated to the rise of MBE pressure. On the contrary, during the deposition of Sb, we observed a reduction of the absolute value of photocurrent. Since the QE is  $\sim 0$  % as this step, this decrease may be associated to noise and/or pressure variations.

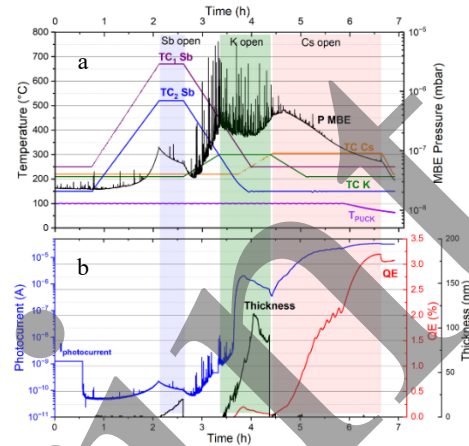


Figure 3: a. Evolution of the MBE pressure vs time regarding temperature synthesis of the 1<sup>st</sup> photocathode and b. Evolution of photocurrent, thickness and QE vs time.

Moreover, during K deposition, the absolute value of photocurrent as well as the QE rapidly increased, meaning a K<sub>2</sub>Sb phase was created. Then, a decrease is observed, which can be correlated to a potassium excess [4].

Finally, during Cs deposition, the absolute value of photocurrent reached 30  $\mu$ A and the QE achieved a value close to 3 % after a small decrease. This decrease in QE was observed when reducing the Cs source temperature, suggesting that the photocathode was operating near its optimal caesium coverage. The reduction of Cs flux may have led to a deviation from the optimal surface stoichiometry, resulting in a decrease in photoemission. Moreover, it should be noted that the thickness could not be measured during Cs deposition due to a software issue. Furthermore, this photocathode was synthesized with a moderate vacuum due to an accidental air leak. As a consequence, the QE dropped to 1 % within a day and to 0 % three weeks later. As a result, a very poor dark lifetime was observed due to bad vacuum conditions.

A second photocathode was synthesised using the same parameters, after a bakeout out of the MBE chamber, ensuring a pressure  $< 10^{-9}$  mbar. However, we were not able to perform it in one process. Fig. 4.a. shows the evolution of the chamber pressure during the evaporator heating and the deposition process. As for the first photocathode, the pressure increased with the temperature, from  $\sim 4 \cdot 10^{-9}$  mbar to  $\sim 9 \cdot 10^{-8}$  mbar. This is related to degassing of antimony. Fig. 4. b. reveals a QE close to 0 % and slight variations of the absolute photocurrent which is in the range of nA. This corresponds to noisy signals.

The heating of K evaporator revealed, as similarly observed, a pressure rise with the temperature, from  $4 \cdot 10^{-9}$  mbar to  $\sim 8 \cdot 10^{-8}$  mbar (Fig. 5. a), responsible of outgassing. During the deposition of K and Cs, the pressure remains

between  $5 \cdot 10^{-8}$  and  $10^{-7}$  mbar, which corresponds to a better pressure than that of the 1<sup>st</sup> photocathode thanks to the second bakeout.

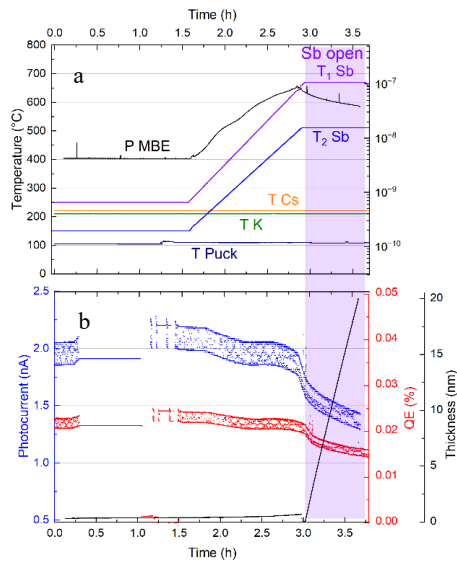


Figure 4: a. Evolution of the MBE pressure vs time regarding temperature synthesis and b. Evolution of photocurrent, thickness and QE vs time during Sb deposition.

Fig. 5. b. shows a two-step increase in the absolute photocurrent during the K deposition. This two-step evolution is not explained since it does not seem to be related to the temperature or pressure variation. However, it is in agreement with the creation of a K<sub>2</sub>Sb phase. The further decrease is attributed to a K excess. Introducing an apparent K excess should be ideal to get the 1:2:1 stoichiometry but leads to a slight improvement of QE [9].

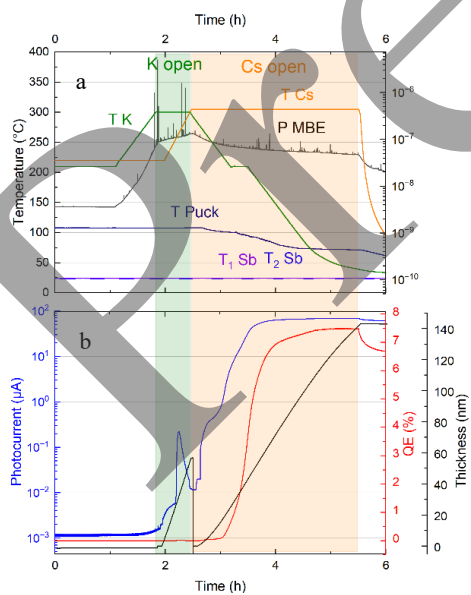


Figure 5: a. Evolution of the MBE pressure vs time regarding temperature synthesis and b. Evolution of photocurrent, thickness and QE vs time during K and Cs deposition.

Finally, during Cs deposition, we observed a strong increase of the absolute value of photocurrent until a plateau

of  $\sim 70 \mu\text{A}$ . The QE was found to strongly increase during this process until a plateau of 7.5 %. When the Cs evaporator started to cooled down, a small drop of photocurrent and of QE is observed to 60  $\mu\text{A}$  and 6.7 % respectively. These two values are higher than those obtained for the first photocathode, which confirms the influence of the vacuum conditions on the photocathode performance. Moreover, even after three weeks, the QE has fallen but is slightly higher than 5 %, which confirms that this photocathode was synthesized in better vacuum conditions. As a result, a dark lifetime higher than 150 hours was reached.

## CONCLUSION

In this paper we report the synthesis of CsK<sub>2</sub>Sb photocathodes for PERLE high current DC-gun, prepared by a sequential evaporation. The quantum efficiency was found to strongly depends on the vacuum quality. A first photocathode synthesized in a vacuum of tens of  $10^{-7}$  mbar exhibit a moderate QE around 3 %. Improving the vacuum quality is found to enhance the QE up to 6.7 %. These preliminary results are encouraging for future electron beam studies and should be correlated to chemical analyses.

## REFERENCES

- [1] B. Dunham *et al.*, “Record high-average current from a high-brightness photoinjector”, *Appl. Phys. Lett.*, vol. 102, no. 034105, pp. 1-4, 2013. doi:10.1063/1.4789395
- [2] S. Schubert *et al.*, “Bi-alkali antimonide photocathodes for high brightness accelerators”, *APL Mater.*, vol. 1, no. 032119, pp. 1-6, 2013. doi:10.1063/1.4821625
- [3] A. di Bona *et al.*, “Development, operation and analysis of bialkali antimonide photocathodes for high-brightness photoinjectors”, *Nucl. Instr. and Meth. in Phys. Res. A*, vol. 385, no. 3, pp. 385-390, 1997. doi:10.1016/S0168-9002(96)00809-1
- [4] H. Panuganti *et al.*, “Synthesis, surface chemical analysis, lifetime studies and degradation mechanisms of Cs-K-Sb photocathodes”, *Nucl. Instr. and Meth. in Phys. Res. A*, vol. 986, no. 164724, pp. 1-10, 2021. doi:10.1016/j.nima.2020.164724
- [5] L. Guo *et al.*, “Substrate dependence of CsK<sub>2</sub>Sb photocathode performance”, *Prog. Theor. Exp. Phys.*, vol. 033G01, pp. 1-10, 2017. doi:10.1093/ptep/ptx030
- [6] M. A. Mamun *et al.*, “Correlation of CsK<sub>2</sub>Sb photocathode lifetime with antimony thickness”, *APL Mater.*, vol. 3, no.066103, pp. 1-7, 2015. doi:10.1063/1.4922319
- [7] G. Blokesch *et al.*, “Test of a DC-photogun injector for the Lighthouse facility”, *J. Phys.: Conf. Ser.*, vol. 2687, no. 032037, pp. 1-6, 2024. doi:10.1088/1742-6596/2687/3/032037
- [8] J. R.Arthur, “Molecular Beam Epitaxy”, *Surf. Sci.*, vol. 500, no. 1-3, pp. 189-217, 2002. doi:10.1016/S0039-6028(01)01525-4
- [9] L. Guo *et al.*, “Improved robustness of sequentially deposited potassium cesium antimonide photocathodes achieved by increasing the potassium content towards theoretical stoichiometry”, *Sci.Rep.*, vol. 15, no. 2900, pp. 1-9, 2025. doi:10.1038/s41598-025-87603-6